

## Interpreting the Dynamic Interaction between a Very Small Rising Bubble and a Hydrophilic Titania Surface

Journal:	<i>The Journal of Physical Chemistry Letters</i>
Manuscript ID:	Draft
Manuscript Type:	Letter
Date Submitted by the Author:	
Complete List of Authors:	Manica, Rogerio; Institute of High Performance Computing, Large-Scale Complex Systems Parkinson, Luke; Ian Wark Research Institute Ralston, John; University of South Australia, Ian Wark Research Institute Chan, Derek; Particulate Fluids Processing Ctr., Dept. of Mathematics & Statistic



# Interpreting the Dynamic Interaction between a Very Small Rising Bubble and a Hydrophilic Titania Surface

Rogério Manica<sup>1</sup>, Luke Parkinson<sup>2</sup>, John Ralston<sup>2</sup> and Derek Y.C. Chan<sup>3,4\*</sup>

<sup>1</sup>Institute of High Performance Computing, 1 Fusionopolis Way,  
#16-16 Connexis, 138632 Singapore

<sup>2</sup>Ian Wark Research Institute, University of South Australia,  
Mawson Lakes SA 5095, Australia

<sup>3</sup>Particulate Fluids Processing Centre, Department of Mathematics and Statistics,  
The University of Melbourne, Parkville VIC 3010 Australia

<sup>4</sup>Department of Mathematics, National University of Singapore, 117543 Singapore

\* Email: D.Chan@unimelb.edu.au

We interpret recent measurements of time-varying interference fringe intensities observed between rising bubbles (diameter 15–120  $\mu\text{m}$ ) and a horizontal hydrophilic titania surface. The bubbles remain spherical because of small buoyancy forces and high Laplace pressures. The theory is based on Stokes flow and the approach velocity is determined from the balance of buoyancy force, hydrodynamic force due to the drainage of the water thin film between the bubble and the titania surface and surface forces – van der Waals and electric double layer interactions. The results are consistent with the no-slip hydrodynamic boundary condition at the surface of the bubble and the titania surface, although far from the surface the terminal velocity of the rising bubbles are consistent with fully mobile bubble surfaces with zero tangential stress.

Parkinson and Ralston<sup>1</sup> reported detailed measurements of the dynamics of the approach of single bubbles (15–120  $\mu\text{m}$  in diameter) rising under buoyancy force in an aqueous electrolyte towards a smooth horizontal titania plate. The experimental data were in the form of high-speed recordings (1000 frames per second) of time varying interference fringes between the bubble surface and the titania surface as the

1  
2  
3 bubble approached. From the intensity pattern of these fringes, it is possible to infer  
4 the shape of the bubbles and the time variation of the separation between the bubble  
5 and titania plate with a resolution to better than 10 nanometers. A related technique  
6 has been used recently to quantify the deformations and the separation between a  
7 mercury drop and a surface<sup>2,3</sup> and between approaching drops in various liquids<sup>4,5</sup>.  
8 The electrical double layer interaction between the titania plate and the bubble can be  
9 controlled by changing electrolyte concentration, and adjusting the pH above and  
10 below the titania isoelectric point permits the sign of the titania surface charge to be  
11 reversed. Our goal is to develop a theoretical model to interpret these measurements  
12 and to quantify the parameters that determine dynamic bubble-surface interaction in  
13 this system.  
14  
15  
16  
17  
18  
19  
20  
21  
22

23 Under identical solution conditions, results of terminal rise velocity  
24 measurements are consistent with the bubble surface being a fully mobile interface  
25 that cannot support any shear stress and, as such, the terminal velocity obeys the  
26 Hadamard-Rybczynski formula<sup>6</sup>. However, it has been observed that even small  
27 traces of surfactant in the system are enough to cause the bubble surface to behave as  
28 an immobile (no-slip) interface<sup>6-9</sup>. One objective of our modeling is to investigate the  
29 boundary condition that holds at the liquid-vapor interface when the bubble is close to  
30 the surface. Comparisons between theory and experiments are performed for a matrix  
31 of experimental conditions at pH 6.3 (repulsive double layer between the bubble and  
32 the surface), two different salts: KCl and N(CH<sub>3</sub>)<sub>4</sub>Br for five different concentrations  
33 ranging from no salt to 10<sup>-1</sup> M. For each case the results corresponding to at least  
34 three bubbles of different diameters were analyzed.  
35  
36  
37  
38  
39  
40  
41  
42  
43

44 In the experimental apparatus a bubble of radius  $R$  is allowed to rise under  
45 gravity before striking a transparent titania (TiO<sub>2</sub>) surface. Readers are referred to  
46 Parkinson and Ralston<sup>1</sup> for details of the experiments. The goal is to deduce time  
47 variations of the distance of closest approach,  $h(t)$  between the bubble and the surface.  
48 The interference fringes between the titania/electrolyte and the air/electrolyte  
49 interface are recorded using a high-speed camera at 1000 fps. Time variations of the  
50 intensity  $I(t)$  at the centre of the fringe pattern can be converted to the distance of closest  
51 approach  $h(t)$  between the bubble and the titania surface through the following relation<sup>10</sup>  
52  
53  
54  
55  
56  
57

$$\frac{I(t) - I_{\min}}{I_{\max} - I_{\min}} = \sin^2 \left( \frac{2\pi n h(t)}{\lambda_0} \right) \quad (1)$$

where  $I_{\max}$  and  $I_{\min}$  are the maximum and minimum intensity respectively,  $\lambda_0$  (550 nm) the wavelength of light in air and  $n$  (1.333) is the refractive index of water.

The radii of the bubbles were kept to below 60  $\mu\text{m}$  to ensure that the Reynolds number ( $Re = 2\rho R V_{St}/\mu$ ) does not exceed 1, where  $\rho$  is the density,  $\mu$  the viscosity of water and  $V_{St}$  the terminal rise velocity calculated from the Stokes formula:  $V_{St} = (2/9)(\rho R^2 g/\mu)$  where  $g$  is the acceleration due to gravity. Therefore Stokes flow is appropriate for this system and we can introduce surface forces to the Brenner solution of a sphere approaching a horizontal surface<sup>11</sup> to model the rise of the bubble towards the titania plate under the influence of hydrodynamic and colloidal surface forces. If the air/water interface of the bubble is immobile and the no-slip hydrodynamic boundary condition applies then equating forces on the bubble gives

$$6\pi\mu R\beta(h)\frac{dh}{dt} = -\frac{4}{3}\pi R^3\rho g + 2\pi R[E_{vdW}(h) + E_{EDL}(h)] \quad (2)$$

The LHS of eq 2 is the hydrodynamic drag force  $F_d$  with  $\beta(h)$  given by eq 2.19 of Brenner<sup>11</sup>. The first term on the RHS is the buoyancy force,  $E_{vdW}$  and  $E_{EDL}$  are respectively the van der Waals and electrical double layer interaction energy per unit area between the bubble and the titania surface and they are related to the corresponding force via the Deryaguin approximation. The bubble ultimately reaches a final equilibrium separation  $h_{eq}$  determined solely by surface forces when  $dh/dt = 0$ . The drag force has two well-known limiting cases: when the bubble is far from the plate ( $h/R \rightarrow \infty$ ),  $\beta(h) \rightarrow 1$  and we have the Stokes law  $F_d = -6\pi\mu R (dh/dt)$ ; and when the separation is small ( $h/R \rightarrow 0$ ),  $\beta(h) \rightarrow R/h$  and we have the Taylor limit  $F_d = -6\pi\mu(R^2/h) (dh/dt)$ . In this limit, eq 2 becomes

$$\frac{6\pi\mu R^2}{h} \frac{dh}{dt} = -\frac{4}{3}\pi R^3\rho g + 2\pi R[E_{vdW}(h) + E_{EDL}(h)]. \quad (3)$$

In the case of high salt concentration in which electrical double-layer interaction ( $E_{EDL}$ ) can be neglected, the repulsive van der Waals interaction (without electromagnetic retardation effects) is  $E_{vdW} = -A/(12\pi h^2)$ , with Hamaker constant  $A = -4. \times 10^{-20} \text{ J} < 0$  for  $\text{TiO}_2/\text{water}/\text{air}$  Eq 3 can be easily integrated to give variations of the bubble-titania separation as a function of time:

$$h(t) = \sqrt{\eta^2 + (h_0^2 - \eta^2)e^{-2t/\tau}} \quad (4)$$

where  $h_0$  is the initial separation,  $\eta^2 = |A|/(8\pi\rho g R^2)$  and  $\tau = 9\mu/(2\rho g R)$ .

The electrical double layer interaction free energy per unit area can be calculated from the superposition approach for  $\kappa h > 2$  as<sup>12</sup>

$$E_{EDL} = \frac{64n_o kT}{\kappa} \tanh\left(\frac{y_1}{4}\right) \tanh\left(\frac{y_2}{4}\right) e^{-\kappa h} \quad (5)$$

where  $n_o$  is the number concentration of 1:1 electrolyte,  $k$  the Boltzmann constant,  $T$  the temperature,  $1/\kappa$  the Debye length and  $\Psi_i = kTy_i/e$ , ( $i = 1,2$ ) is the surface potential on the bubble or on the titania plate. As we shall see, the equilibrium film thicknesses,  $h_{eq}$  are always larger than the Debye length ( $\kappa h_{eq} > 1$ ) which justifies the use of eq 5. Furthermore in the superposition limit, we need not be concerned with whether the surfaces interact under constant surface charge or surface potential.

A comparison of the relative magnitudes of different forces acting on the bubble is given in Figure 1 at pH 6.3 where the electrical double layer interaction is repulsive. For low salt concentrations, the electrical double layer interaction dominates, so for instance, the equilibrium separation between a bubble with a radius of 40  $\mu\text{m}$  and the surface at 1 mM salt is given by point A in Figure 1. At high salt concentrations, the van der Waals repulsion dominates and the equilibrium position for example of a bubble with a radius of 10  $\mu\text{m}$  radius at 0.1 M salt is indicated by point B in Figure 1. Intermediate concentrations generally require the consideration of both forces as for example a bubble with a radius of 20  $\mu\text{m}$  radius at 0.01 M.

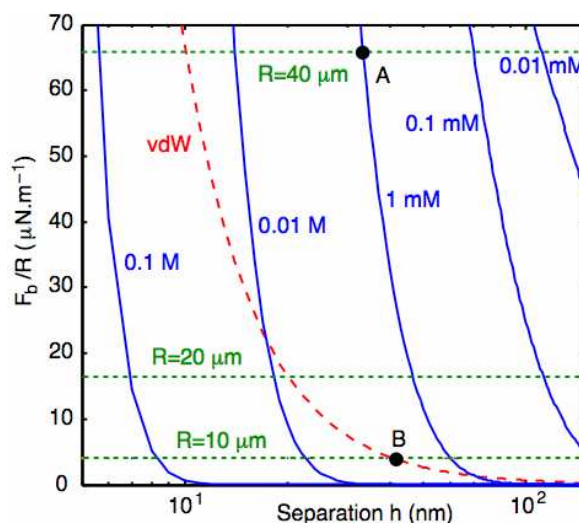


Figure 1. Forces on a bubble: van der Waals interaction (---) with Hamaker constant  $A = -4 \times 10^{-20}$  J and electrical double layer interaction (—) for  $10^{-5}$  to  $10^{-1}$  M 1:1 electrolyte and surface potentials  $\Psi = -45$  mV (titania)<sup>1</sup> and  $-60$  mV (bubble)<sup>13</sup>. The buoyancy force,  $F_b = (4\pi/3) \rho g R^3$  (- - -) for 3 different bubble radii is also plotted.

1  
2  
3  
4  
5  
6  
7  
8  
9  
10  
11  
12  
13  
14  
15  
16  
17  
18  
19  
20  
21  
22  
23  
24  
25  
26  
27  
28  
29  
30  
31  
32  
33  
34  
35  
36  
37  
38  
39  
40  
41  
42  
43  
44  
45  
46  
47  
48  
49  
50  
51  
52  
53  
54  
55  
56  
57  
58  
59  
60

We first consider the fringe intensity of a bubble resting at its equilibrium position after it has risen to the titania plate. In Figure 2 we compare the form of experimental fringe intensity (left side) with the theoretical intensity (right side) calculated using eqs (1) and (2) for a bubble resting at the plate at an equilibrium separation  $h_{eq}$  determined by a balance of buoyancy and electrical double forces ( $h_{eq} = 20$  nm). The bubble surface is assumed to be spherical, with  $h(r) = h_{eq} + r^2/(2R)$ , where  $R = 50$   $\mu\text{m}$  is the measured bubble radius. We see excellent agreement using measured system parameters as input to the theory. As this comparison is for one of the largest bubbles in the experimental range, we are confident that the smaller bubbles were also spherical and not deformed as a result of interactions.

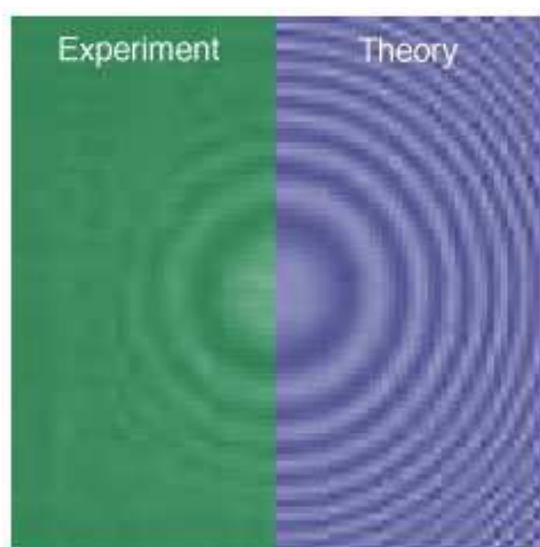


Figure 2. Snapshot of the experimental intensity fringes (LHS) with resolution of  $0.34$   $\mu\text{m}$  per pixel compared to theoretically generated fringes (RHS) for a bubble at equilibrium against the titania plate in  $0.1$  M  $\text{N}(\text{CH}_3)_4\text{Br}$  electrolyte. The bubble radius is  $50$   $\mu\text{m}$ , the surface potentials are  $-45$  mV (titania)<sup>1</sup> and  $-60$  mV (bubble)<sup>13</sup> and the equilibrium separation is  $h_{eq} = 20$  nm.

From eq 1, we see that the rate of approach of the bubble towards the titania plate is related to the time variation of the intensity at the centre of the fringe pattern. We therefore model this variation using two extreme models for the hydrodynamic boundary condition at the bubble surface: an immobile interface that obeys the “no-slip” boundary condition and the bubble behaves hydrodynamically like a solid particle, or a tangentially mobile interface that will not support any shear stress. The results in Figure 3a and 3b for a bubble at  $0.1$  mM KCl approaching the titania surface demonstrates unambiguously that time variations of the central fringe intensity  $I(t)$  (Figure 3a) or equivalently, time variations of the separation  $h(t)$  between the bubble and the titania plate (Figure 3b)

coincides with the theoretical predictions for an immobile (“no-slip”) condition at the air/water interface of the bubble surface. The key observation is the excellent agreement between experiments and the predictions of the “no-slip” boundary condition for the periodicity of the intensity oscillations that reflects directly the rate of film thinning. The slightly lower amplitudes in the intensities at early times are due to attenuation and scattering by the thicker film. The results in Figure 3c and 3d demonstrate that modeling the primary intensity data, and in particular the periodicity of the intensity variation, provides a more sensitive test between experiment and theory than modeling the monotonically decreasing separation  $h(t)$ . For instance, the disagreement between theoretical and experimental intensity at large times is quite marked while the corresponding difference in the equilibrium separation  $h_{eq}$  appears rather small. Predictions using the fully mobile instead of the “no-slip” boundary condition at the bubble surface for Figs 3c and 3d give similar results as in Figs 3a and 3b in that the period of the oscillations in the intensity is too short and thus the separation  $h(t)$  decreases too rapidly.

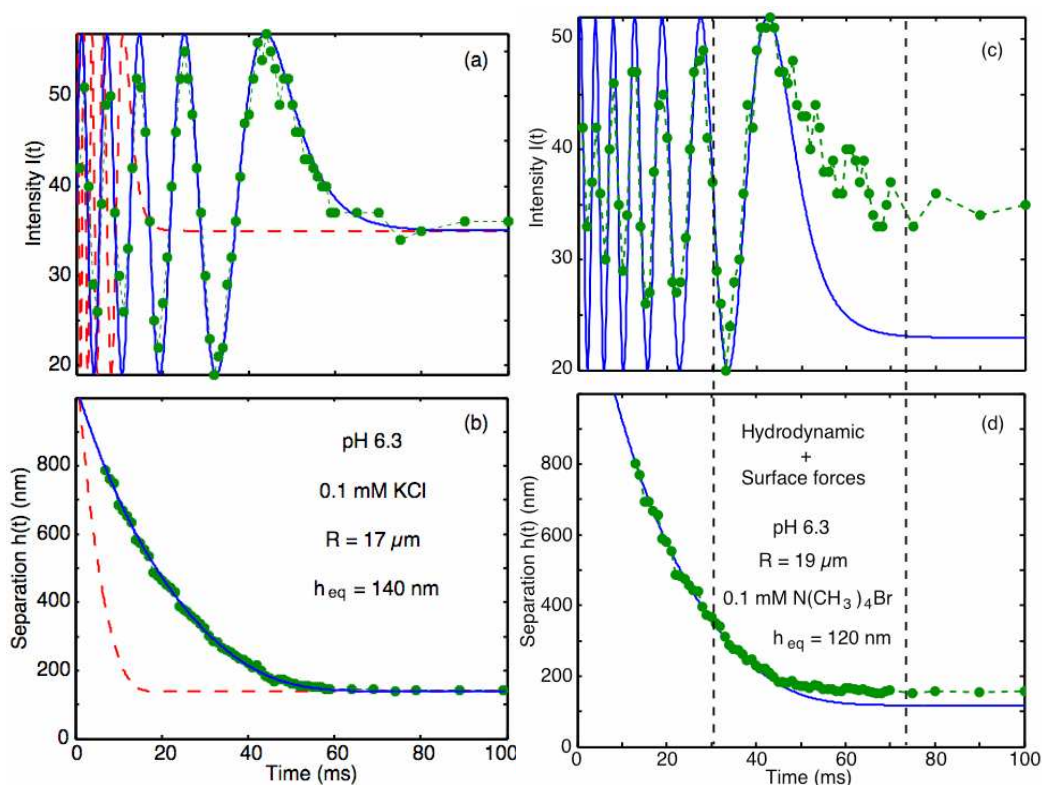


Figure 3. Comparison between theory and experiment using the immobile (“no slip”) (—) and fully mobile (- - -) boundary conditions at the bubble surface for (a) the fringe central intensity and (b) the corresponding separation at 0.1 mM KCl. Similar comparison for 0.1 mM  $\text{N}(\text{CH}_3)_4\text{Br}$  are in (c) and (d). The surface potential surface potentials are taken to be  $-45$  mV (titania)<sup>1</sup> and  $-60$  mV (bubble)<sup>13</sup>.

1  
2  
3  
4  
5 Comparisons between theory and experiment for most bubbles studied showed  
6 that the rate of approach of the bubble towards the titania plate at small times when  
7 hydrodynamic effects dominate, is consistent with the immobile “no-slip” hydrodynamic  
8 boundary conditions using values of bubble radii that are within the experimental  
9 uncertainty of 2  $\mu\text{m}$  of the measured bubble sizes. However, measurement of bubble  
10 terminal velocity prior to any interaction with the titania surface showed results that were  
11 accurately predicted by the Hadamard-Rybczynski formula, which is derived under the  
12 assumption of a tangentially mobile bubble surface. Possible reasons for the observed  
13 change in boundary condition have been proposed<sup>1</sup>.  
14  
15  
16  
17  
18  
19  
20

21 The results in Figure 3 (c) and (d) also illustrate the different separation regimes  
22 of the bubble-plate interaction. In this particular example only hydrodynamic effects are  
23 important for times smaller than 30 ms when the separation is sufficiently large that the  
24 influence of surface forces may be neglected. For time larger than 70 ms only surface  
25 forces are important because the bubble is almost stationary and so there are no  
26 hydrodynamic effects. At intermediate times, between 30 – 70 ms, both hydrodynamic  
27 and surface force effects combine to influence the motion of the bubble.  
28  
29  
30  
31  
32  
33

34 Over 60 experimental data sets have been analyzed with satisfactory agreement  
35 for different salts, concentrations and bubble sizes. The cases of low electrolyte  
36 concentrations where double layer interactions are dominant and equilibrium separations  
37 are large gave better agreement overall compared to the cases of small equilibrium  
38 separations. We selected one representative case of each electrolyte concentration and  
39 present the results in Figure 4. As the concentration is increased the equilibrium thickness  
40 decreases, which is expected since the electrical double layer becomes shorter ranged  
41 with increasing electrolyte concentration, see Figures 4a – 4c. In these cases, the  
42 intensities at large times are determined mainly by the electrolyte concentration. The  
43 rather small effects at large times due to variations of the bubble surface potentials  
44 between –30 to –100 mV are indicated by the error bars. At very low salt concentration  
45 (Figure 4a), the surface potential and the unknown salt concentration are treated as fitting  
46 parameters: –60 mV and  $3.5 \times 10^{-6}$  M. But, the same parameters will reproduce measured  
47 intensities from the same batch of bubbles. At 0.1M salt (Figure 4d), the equilibrium  
48 thickness is determined only by repulsive van der Waals interactions between the bubble  
49 and the titania surface since all electrostatic interactions are screened out. This is a  
50  
51  
52  
53  
54  
55  
56  
57  
58  
59  
60

practical instance of repulsive Lifshitz-van der Waals interactions that has attracted recent interest in the context of quantum levitation<sup>14</sup>.

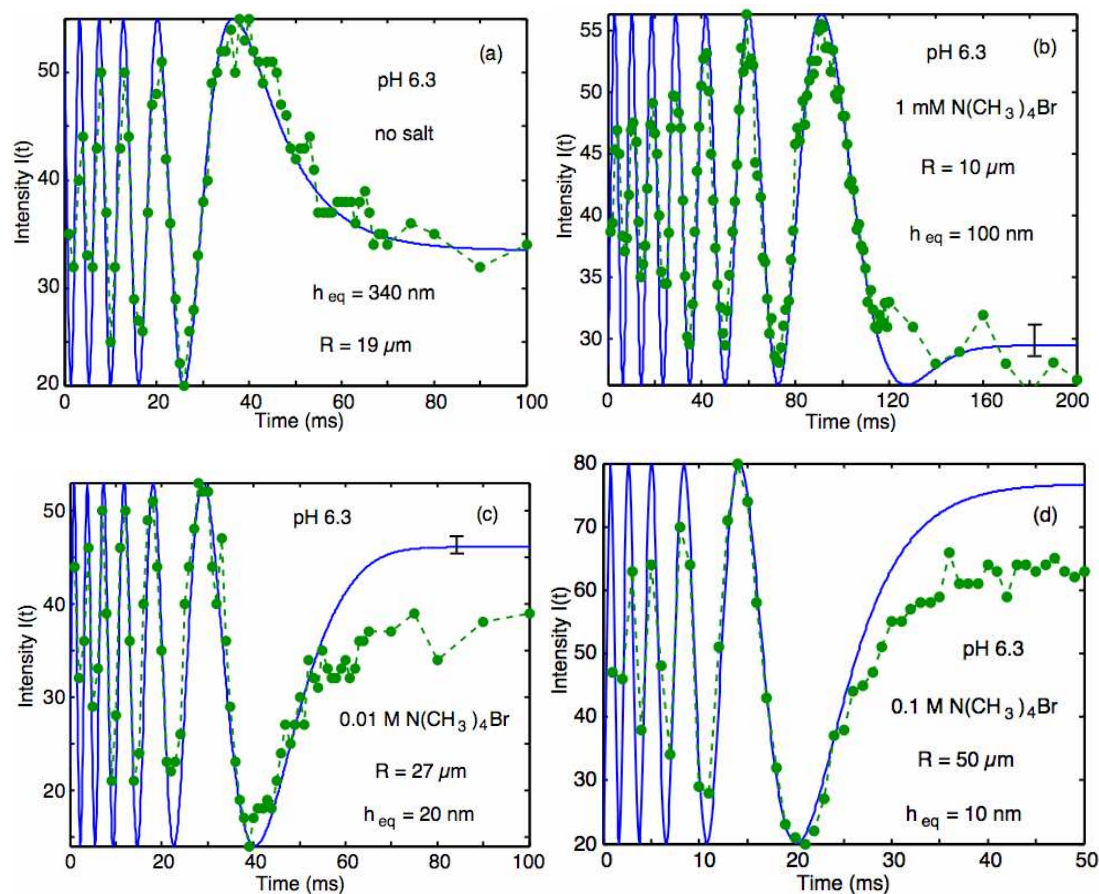


Figure 4. Comparison between theory and experiment for different salt concentrations ranging from no salt added to 0.1 M. Details of each experiment are given in the figure. The surface potential of the titania and bubble surfaces are taken to be  $-45$  mV and  $-60$  mV respectively.

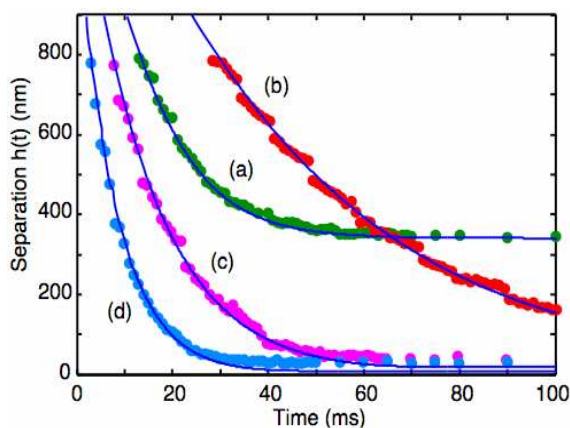


Figure 5. Bubble-titania plate separation  $h(t)$  corresponding to the intensity functions of Figure 4. The labels (a) – (d) of the theoretical curves and experimental data points refer to the plots in Figure 4.

1  
2  
3  
4  
5 The time evolution of the bubble position  $h(t)$  that corresponds to the results in  
6 Figure 4 are presented in Figure 5 with curves (a) – (d) matching the respective plots in  
7 Figure 4. These results demonstrate that the rate of approach of the bubbles to the titania  
8 surface increases with bubble radius due to the larger buoyancy forces and illustrate the  
9 importance of electrolyte concentration on the equilibrium position of the bubbles.  
10

11  
12  
13  
14 The theory presented in this paper is successful in providing an accurate  
15 description of small bubbles rising under gravity under Stokes flow. It combines in one  
16 model the 3 different phases of interaction that arise (i) from hydrodynamic drag when  
17 the bubble is far from the titania plate, (ii) at intermediate separations from both  
18 hydrodynamic interactions, given by the Brenner theory and surfaces forces represented  
19 by electrical double layer and van der Waals interactions that retard the bubble and finally  
20 (iii) near equilibrium where only surface forces are relevant in determining the  
21 equilibrium separation. The theory compares well against the experimental data for all  
22 times and is flexible enough to be adapted to similar systems with different surfaces  
23 forces or boundary conditions.  
24  
25  
26  
27  
28  
29  
30

31  
32 The primary experimental results are the measured intensity data of the  
33 interference fringes and our theoretical approach in analyzing the experimental data is  
34 therefore to model the evolution of the fringe intensities directly. This proved to be a  
35 sensitive test between experiment and theory. Furthermore, measuring the periodic time  
36 variation in a reflected light interference pattern is a sensitive way to deduce the  
37 separation between the bubble and the surfaces.  
38  
39  
40  
41

42 The immobile boundary condition for the air-water interface provided the best  
43 agreement between theory and experiments even though the initial bubble rise velocity  
44 appears consistent with a fully mobile interface. While extreme care has been taken to  
45 ensure cleanliness in our experimental system as demonstrated by bubble rise velocities  
46 being consistent with a fully mobile bubble surface, we cannot completely rule out  
47 possibility of contamination in the solution in the close proximity of the titania surface.  
48 Trace amounts of surface-active contaminants are sufficient to arrest hydrodynamic  
49 mobility at the bubble surface and cause the “no-slip” to hold at the bubble surface<sup>8,9</sup>.  
50  
51  
52  
53  
54  
55  
56  
57  
58  
59  
60

1  
2  
3 Financial support from the Australian Research Council Linkage Grants Scheme and  
4 AMIRA International is gratefully acknowledged. RM thanks the University of  
5 Melbourne and IHPC for supporting the travel to Australia that originated this work.  
6  
7  
8  
9

- 10  
11  
12 (1) Parkinson, L.; Ralston, J. J. *Phys. Chem. B.* (submitted) ID: jp-2009-06259x.  
13  
14 (2) Connor, J. N.; Horn, R. G. *Faraday Discuss.* **2003**, *123*, 193.  
15  
16 (3) Manica, R.; Connor, J. N.; Carnie, S. L.; Horn, R. G.; Chan, D. Y. C. *Langmuir*,  
17 **2007**, *23*, 626.  
18  
19 (4) Klaseboer, E.; Chevaillier, J. Ph.; Gourdon, C.; Masbernat, O. *J. Colloid Interface*  
20 *Sci.* **2000**, *229*, 274.  
21  
22 (5) Manica, R.; Klaseboer, E.; Chan, D.Y.C. *Soft Matter*, **2008**, *4*, 1613.  
23  
24 (6) Parkinson, L.; Sedev, R.; Fornasiero, D.; Ralston, J. J. *Colloid Interface Sci.*  
25 **2008**, *322*, 168.  
26  
27 (7) Kelsall, G. H.; Tang, S.; Smith, A. L.; Yurdakul, S. *J. Chem. Soc., Faraday Trans.*  
28 **1996**, *92*, 3879.  
29  
30 (8) Manor, O.; Vakarelski, I. U.; Tang, X.; O'Shea, S. J.; Stevens, G. W.; Grieser, F.;  
31 Dagastine, R. R.; Chan, D. Y. C. *Phys. Rev. Lett.* **2008**, *101*, 24501.  
32  
33 (9) Manor, O.; Chan, D. Y. C. *Langmuir*, **2009**, *25*, 8899.  
34  
35 (10) Born, M.; Wolf, E. *Principles of Optics*. Cambridge University Press; 6<sup>th</sup> ed. **1997**.  
36  
37 (11) Brenner, H. *Chem. Eng. Sci.* **1961**, *16*, 242.  
38  
39 (12) Hunter, R. J., *Foundations of Colloid Science*, Chapter 7, Oxford University Press,  
40 **1987**.  
41  
42 (13) Yang, C.; Dabros, T.; Li, D.; Czarnecki, J.; Masliyah, J. H. *J. Colloid*  
43 *Interface Sci.* **2001**, *243*, 128.  
44  
45 (14) Munday, J. N.; Capasso, F.; Parsegian, V. A. *Nature*, **2009**, *457*, 170.  
46  
47  
48  
49  
50  
51  
52  
53  
54  
55  
56  
57  
58  
59  
60

## Figures for Table of Contents

